

Sliding Mode Control and Simulation of a Hybrid Fuel-Cell Ultracapacitor Power System

T. Azib, R. Talj, O. Bethoux, *Member, IEEE*, and C. Marchand *Member, IEEE*.
Laboratoire de Génie Electrique de Paris (LGEP) / SPEE-Labs, CNRS UMR 8507,
SUPELEC ; Université Paris Sud VI (UPS11) ; Université Pierre Marie Curie (UPMC).
Plateau de Moulon, 91192 Gif-sur-Yvette cedex,
Toufik.Azib@lgep.supelec.fr

Abstract- This paper deals with a robust control strategy for modern distributed generation systems made up of hybrid PEM (proton exchange membrane) Fuel Cell (FC) and Ultracapacitors (UCs) power system. Particularly, for future fuel cell a vehicle application is presented. Given the constraint of the FC dynamics and the complexity of the energy management, a second order sliding mode control (SMC) strategy is designed to improve the robustness and the performance of the system. This control strategy, based on frequency decomposition of the load specifications, uses a cascaded closed loop control. It takes into account the slow dynamics of FC and the state of charge (SOC) of the UCs. FC output power is determined according to the low frequency (LF) load requirement and the UC SOC. UCs value is determined according to the high frequency (HF) load requirement. Therefore, two voltage control loops are designed. The DC bus voltage is regulated by the UCs source using a classical proportional integrator (PI) controller. The UCs SOC voltage is regulated by the FC source using a sliding mode (SM) controller, which improves the global performance of the controlled system.

An analysis of the simulation results is conducted using Matlab/Simulink software in order to verify the effectiveness of the proposed control strategy. It confirms that the developed model and its control strategy exhibit excellent performance.

I. INTRODUCTION

Fuel Cell Vehicle (FCV) is a promising fuel cell application that has taken more and more importance in the last years. It has the potential to substantially reduce emissions and increase engine efficiency [1], [2]. Among the various fuel cell technologies, the polymer electrolyte membrane (PEM) fuel cell is considered as the most promising one to replace the combustion engine because of its capability of high power densities, low operating temperatures, lightweight nature, small size, and short start-up time [2]. Integrating a single fuel cell system into a vehicular power train, is not always sufficient to supply propulsion power for a vehicle which is characterized by load profiles with high ratios of peak power to average power. Indeed, FC systems have some deficiencies linked to their inherent characteristics, such as high cost, poor time response to instantaneous power demands due to the low time response of the air delivery system, and no regenerative energy

recovery during braking [3], [4]. Consequently, erratic load power demand may lead to fuel cell starvation phenomena thus decreasing its performance and lifetime [5]. Hybridization of a fuel cell system with energy storage devices can be a solution to these drawbacks. Hybridization is relevant because the energy storage device is able to provide instant peak power during transient conditions of vehicle operation and also to improve fuel economy by storing the regenerative braking power [6]. At the present time, this auxiliary device can be either batteries or ultracapacitors (UCs). In comparison to standard batteries, UCs benefit from good energy effectiveness, high power density and high lifetime (more than one million cycles). Another advantage of the UCs consists in operating even at low temperatures (e.g. -20 °C) and in severe thermal constraints. Ultracapacitors are electrical energy storage devices (a few Farads to several thousand Farads per cell) with high power densities when compared with batteries [7], [8].

That is the reason why, the idea is to combine FC with UC, thus creating a Fuel Cell Hybrid Vehicle (FCHV). In such hybrid FC/UCs power source, the fuel cell is controlled to satisfy load average power requirements over a long term period; whereas the transient power requirement, involving important exchanges of power in short time intervals, are ensured by the UCs. Therefore, proper energy management strategy is important to achieve power requirement, maintain the UC SOC, respect slow dynamic of FC and also ensure the safe and durable operation of the global system.

The objective of this work is to develop an efficient energy management strategy of the different sources supplying the load. The proposed strategy is based on the regulation of the DC bus voltage and uses the natural frequency decoupling of each source. Therefore, an imbricate control loop structure is designed. The inner loop controls the DC bus voltage using a PI controller, while the outer loop regulates the SOC of the UCs using a sliding mode (SM) controller. Two different strategies for the latter are presented: first order and second order SM. Some simulation tests are carried out in order to show the effectiveness of the proposed energy management strategy, the good performance of the fuel cell hybrid bus, and the improvement provided by the use of the second order SM strategy.

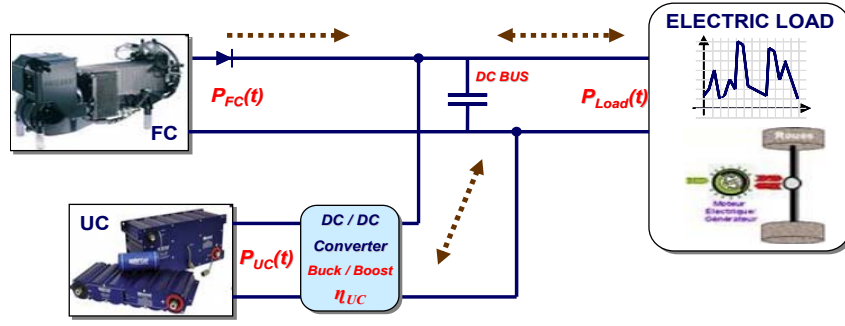


Fig. 1. Hybrid FC/UC configuration.

II. HYBRID FUEL-CELL/ULTRACAPACITOR POWER SYSTEM

A. Description of Hybrid FC/UC Power Systems

Fig. 1 shows the configuration of FC/UC hybrid power system. The hybrid system consists of a fuel cell system, an ultracapacitor pack, a bidirectional DC/DC converter, supervisor controller for energy management strategy, and electrical load emulating the power load profile. The UC pack is connected to the DC voltage bus via the bidirectional DC/DC converter and the FC system is connected directly to the DC voltage bus. Therefore, given a certain load power demand $P_{Load}(t)$, it can be supplied partially from the fuel cell system, $P_{FC}(t)$, the rest of power being supplied by the energy storage system, $P_{UC}(t)$. The power balance in the DC bus must be fulfilled at every time:

$$P_{Load}(t) = P_{FC}(t) + \eta_{UC} P_{UC}(t) \quad \forall t \quad (1)$$

Where η_{UC} is the efficiency of the power converter connecting the UC with the DC bus. We assume that the converter is controlled and its efficiency is known.

B. Modeling of Hybrid FC/UC Power System

1. Fuel Cell model

A FC system consists of many cells connected in series to provide the desired output terminal voltage and current, and exhibits a nonlinear I-V characteristic [9]. Furthermore, the fuel cell system is a complex device with many auxiliary components. Hence, a significant part of the electrical power generated is used internally, which means that the real stack current is greater than i_{FC} . More precisely, the relationship between the FC voltage V_{FC} and the output current i_{FC} is given by the following equations:

$$V_{FC} = N(E_{Cell} - R \cdot j_{Stack} - A \cdot \ln(j_{Stack} + j_l) - m \exp(nj_{Stack})) \quad (2)$$

$$j_{Stack} = \frac{I_{Stack}}{A_{Cell}}, \text{ and here: } I_{Stack} = \alpha + (1 + \beta)I_{FC} + \gamma(I_{FC})^2 \quad (3)$$

The parameters used in the mathematical static model of the FC characteristic are as follows [9]:

- A_{Cell} is the area of each cell,
- N is the stack cell number,
- E_{cell} is the open circuit cell voltage,
- R is the membrane area specific resistance;

A is the Tafel coefficient;
 m, n are the two coefficients of the mass transfer equation

Fig. 2 shows the experimental characteristics and the simulated model of the studied FC (Nexa). This Nexa fuel cell is designed by Ballard. It is of PEM technology, composed of 46 cells and has a nominal power of 1200 W, giving a maximum current of 46 A with voltage of 26 V. The results show that there is an excellent agreement between the measured and simulated values.

2. Ultracapacitors model

Various UCs models can be found in literature, especially for hybrid systems. Classical ultracapacitor theoretical modeling consists of a transmission line [10].

However, to take into account the global ultracapacitor behavior during charge and discharge, a RC model is sufficient to describe the nonlinear electrode behavior:

- The resistor R models the ultracapacitor ohmic losses, usually called equivalent series resistor (ESR).
- The capacitor C represents the ultracapacitor capacitance during charging and discharging effects.

The RC parameter values are extracted directly from the manufacturer's datasheets.

3. Power load profile

The power load specification is mainly due to speed variations, tyre friction dissipation, aerodynamics dissipation and mass elevation. This power, P_{Load} , can be expressed as:

$$P_{motor} = V \left(C_r M g \cos(\alpha) + M g \sin(\alpha) + M \frac{dV}{dt} + \frac{1}{2} \rho S C_x V^2 \right) \quad (4)$$

Where:

- V and M are the vehicle speed and mass (in $m \cdot s^{-1}$ and kg);
- α is the road angle with an horizontal line (in rad);

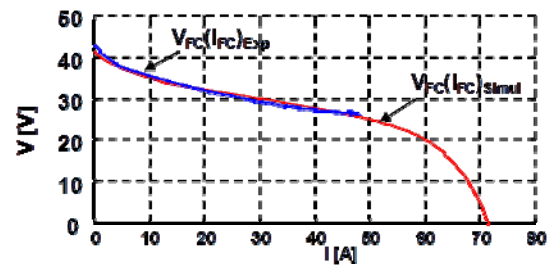


Fig. 2. FC V-I characteristics

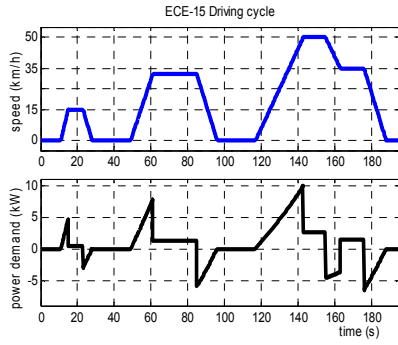


Fig. 3. ECE-15 Driving Cycle.

C_r and C_x are the friction and aerodynamic coefficients;
 ρ is the air density (in $\text{kg}\cdot\text{m}^{-3}$);
 S is the front surface area (in m^2).
 $M=1000$; $g=9,81$; $\alpha=0$; $C_r=0,01$; $C_x=0,30$; $\rho=1,225$; $S=2,5$.

Thus, the vehicle power demand can be determined by the driver's requirements. Indeed, European light duty vehicles have to face the New European Driving Cycle (NEDC) which permits to evaluate and compare the different cars' performances in Europe. The NEDC consists of repeated urban cycles (called ECE-15 driving cycle) and an Extra-Urban driving cycle, or EUDC. Fig. 3 shows the ECE-15 cycle with the speed and the power demand of a car following a flat road.

Sudden power changes can be noticed each time the driver requires a speed change. In this example, the car's average power is only about 0.72 kW, whereas the peak power reaches roughly 10 kW, which means a 13.7 ($P_{\max}/P_{\text{average}}$) ratio. For those reasons, the proposed control strategy is evaluated with a severe profile consisting on raising and falling power edges.

III. ENERGY MANAGEMENT STRATEGY

A. Description

The main motivation for introducing hybridization in fuel cell systems is to solve two important problems in fuel cell control:

- The dynamics of FCs are relatively slow, mainly because of the dynamics of the air compressor.
- The energy storage device (UC) can recover the breaking energy, hence saving primary energy.

Therefore, proper energy management strategy is important to affect these objectives. Thus, the proposed strategy is based on the regulation of the DC bus voltage [11], [12], and uses the natural frequency decoupling of each source (DC bus capacitor, UCs, and FC) as portrayed in Fig. 4 [13]. So, the designed strategy uses a cascaded close loop control allowing a frequency decomposition of the power demand cycle as shown in Fig. 5. Its main principle is based on the use of the UC (the fastest energy source) for supplying the high band of the load power frequency spectrum (HF), thus, avoiding the fuel starvation problem. Conversely, low frequencies (LF) are provided by the fuel cell, which contributes to the long-term autonomy and also maintain the UC state of charge (SOC).

As a result, the energy management strategy leads naturally to a cascaded control loop, as depicted in Fig. 5, with:

- A current closed loop controlling the UC current: to prevent any breaking over-currents or over-voltages, the inner loop is dedicated to UCs current control. This first loop is implemented with a Proportional Integrator (PI) controller with a bandwidth set to 1 kHz.
- The energy management controller (EMC), which contains:
 - A voltage closed loop controlling the DC bus voltage;
 - A compensation closed loop controlling the UC State of Charge (SOC).

B. Energy management controller (EMC)

1. DC bus voltage loop (DCVL)

This strategy ensures the rejection of the load perturbations. Indeed, for every load power demand, the bus voltage is modified. Hence, its measurement is needed for the supervision purposes. As the ultracapacitor modules are able to deliver a large power during a short time, voltage perturbations are taken into account by the UC current (voltage loop). Consequently, the second cascaded loop has to monitor the bus voltage $V_{\text{BUS}}(t)$ and reject the HF load perturbation: faster this voltage tracking, smaller is the C_{BUS} value. This controller can also be built as a Proportional Integrator (PI) controller with a bandwidth set to 100 Hz and an anti-windup block (in order to take into account UC current limitations). The output signal from the regulator must be limited in level, to respect constraints associated with the UC. The closed-loop transfer function of the system (5), deduced from Fig. 5, allows us to determine the parameters K_p and ω_i of the PI controller.

$$H_{CL}(s) = \frac{1}{s + \frac{1}{C_{BUS}S}} \frac{K_p s + \omega_i}{s} = \frac{1 + \tau s}{1 + 2m \frac{s}{\omega_{CL}} + \left(\frac{s}{\omega_{CL}}\right)^2} \quad (5)$$

Where:

$$\omega_{CL} = \sqrt{\frac{\omega_i}{C_{BUS}}}, \quad m = \frac{K_p}{2\sqrt{\omega_i C_{BUS}}} \quad \text{and} \quad \tau = \frac{K_p}{\omega_i} \quad (6)$$

To respect dynamics decoupling, the voltage loop must

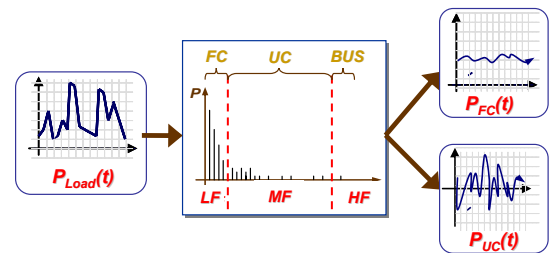


Fig. 4. Bandwidth splitting technique

present a time response ten times larger than the current loop and the desired damping ratio is settled to $m=1$. So, the PI regulator parameters are given:

$$\omega_I = C_{BUS}(\omega_{CL})^2 \quad \text{and} \quad K_P = 2m C_{BUS}\omega_{CL} \quad (7)$$

With, $C_{BUS} = 10 \text{ mF}$ and $f_{CL} = 100 \text{ Hz}$, one computes:

$$\omega_I = 3,95 \cdot 10^2 \text{ rad.s}^{-1}, \quad K_P = 12,6 \quad \text{and} \quad \tau \approx 0,32 \text{ ms} \quad (8)$$

2. SOC compensation loop (SOC CL)

The UC state of charge has to be taken into account by the main supply (FC) in order to maintain it in a suitable range ($V_{Nom}/2 \leq V_{UC} \leq V_{Nom}$). Planning a desired trajectory for $V_{BUS}(t)$ directly prescribes the FC operating point, which is the SOC compensation loop purpose. Nevertheless, the FC characteristic is wrongly known. Thus, to assure a good trajectory of V_{BUS} which respects the slow FC dynamics, a Sliding Mode (SM) controller is used. This controller guarantees a good convergence with perturbation reject [14][15].

The block diagram of the proposed sliding mode controller is presented in Fig. 6, where the sliding surface is defined as:

$$S(t) = \varepsilon(t) + \tau \frac{d\varepsilon(t)}{dt} \quad (9)$$

with $\varepsilon(t) = V_{UC}(t) - V_{UCref}(t)$ and τ a control parameter that determine the rate of convergence of the error (ε) to zero inside the sliding surface $S = 0$.

The real control variable is defined as:

$$V_{BUSref}(t) = \int u dt \quad (10)$$

Given that the real control input V_{BUS} is generated by integrating the variable u , this latter is considered the intermediate control input created by the proposed controller. To generate the variable u , two different control strategies

were designed. The first one suggests the use of a first order sliding mode control with the sliding variable S defined in equation (9). Simulations show a fast transient behavior that can damage the fuel cell, given its slow dynamics requirements. To overpass this constraint, a second order sliding mode – super-twisting algorithm – was designed to insure a robust convergence to the sliding surface ($S = 0$), in finite time, with a suitable dynamics [15], [16].

a. First order sliding mode

The variable u representing $\frac{dV_{BUSref}}{dt}$ is generated by a first order sliding mode control using the sliding variable S already defined,

$$u = -\alpha \text{sign}(S) \quad (11)$$

where α is the control tuning parameter that determine the rate of convergence to the sliding surface.

The parameters α and τ are chosen according to the constraint of a desired bandwidth less than 1 Hz for the FC.

b. Second order sliding mode

To improve the response of the controlled system, and avoid fast transient variations, we looked to use the second order sliding mode control [15], [16].

We noticed that the control input $u = \frac{dV_{BUSref}}{dt}$ appears in the

first derivative of S . Hence, S has a relative degree equal to 1. Indeed,

$$S = (V_{UC} - V_{UCref}) + \tau \frac{-i_{UC}}{C_{UC}} \quad (12)$$

with $\frac{dV_{UC}}{dt} = \frac{-i_{UC}}{C_{UC}}$, and $\frac{dV_{UCref}}{dt} = 0$.

Having the power balance equation as follows

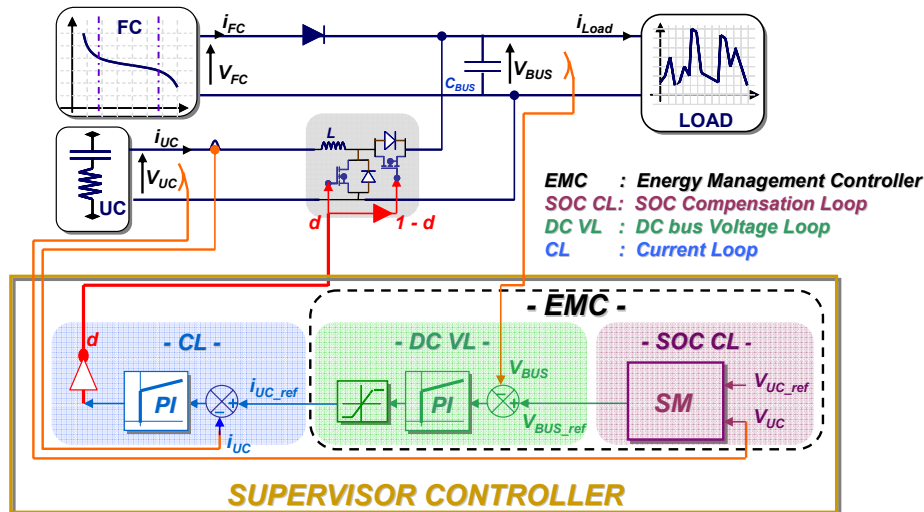


Fig. 5. Control strategy block diagram.

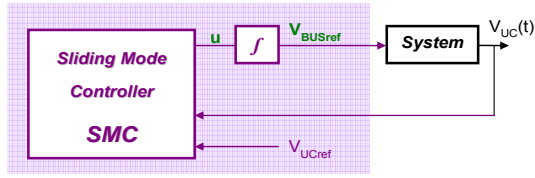


Fig. 6. Sliding Mode Controller

$$V_{UC} i_{UC} = V_{BUS} i_{UC} + L \frac{di_{UC}}{dt} \quad (13)$$

and neglecting the power dissipated in the inductance L , the sliding variable can be expressed as,

$$S = (V_{UC} - V_{UCref}) - \tau \frac{V_{BUS}}{C_{UC} V_{UC}} i_{UC} \quad (14)$$

After some calculation, one can find that the derivative of S can be written as follows

$$\dot{S} = \phi(.) + \varphi(.)u \quad (15)$$

where $\phi(.)$ and $\varphi(.)$ are bounded functions whose expressions are given in [17].

This characteristic of the system motivates us to use the second order sliding mode, super-twisting algorithm, known for its robustness against perturbation and parameters uncertainties.

The input u will be as follows:

$$u(t) = u_1(t) + u_2(t) \quad (16)$$

where

$$\begin{aligned} \dot{u}_1(t) &= -\beta \text{sign}(S) \\ u_2(t) &= -\gamma |S|^\nu \text{sign}(S) \end{aligned} \quad (17)$$

with

$$\beta > \frac{C_0}{k_m}, \quad \gamma^2 \geq \frac{4C_0 k_M (\beta + C_0)}{k_m^3 (\beta - C_0)}, \quad 0 < \nu \leq 0.5 \quad (18)$$

where C_0 , k_m and k_M are constants depending on the system such that

$$|\phi(.)| < C_0, \quad k_m < \varphi(.) < k_M \quad (19)$$

The second order sliding mode control provides one additive degree of freedom, which gives the possibility to better manipulate the controlled system.

The parameters γ , β and τ are tuned also to satisfy the fuel cell dynamics requirements.

IV. SIMULATION RESULTS

The proposed control strategy is evaluated by extensive simulation on the hybrid systems shown in Fig.5, using MATLAB software, Simulink and SimPowerSystems Toolboxes. Table I gives the data used for the simulated system. The results of the simulation are presented mainly in Fig. 7 and 8 for both EMC strategies, using respectively SMC order I and SMC order II. Fig.7, 8 illustrate the operation of

the system throughout a complete load profile (Fig.7-a, Fig.8-a). The power load scenario is described as below:

- From 0 ~20 s, the load does not consume power.
- From 20~40 s, 40~40 s, and 90~120 s, the power load increase from 0~400 W, 400~650 W, and 270~800 W respectively.
- From 70~90 s, 120~160 s, and 160~200 s, the power load decrease from 650~270 W, 800~320 W, and 320~0 W respectively.

When the load power is suddenly increased, the fuel cell power slowly adjusts to the new load level as shown (Fig.7-b, Fig.8-b). During this time, it can be observed on the UCs current (Fig.7-d, Fig.8-d) and power (Fig.7-b, Fig.8-b) that UCs react immediately to supply the transient energy demand which is not supplied by the FC. Thus, FC voltage ($V_{FC}(t)$) is not subjected to any sudden drop which is related to a smooth FC current behaviour ($i_{FC}(t)$) with a 2 A.s⁻¹ slope, as shown in Fig.7-c and Fig.8-c. When the FC output power is sufficient to raise the load requirement, the power flow from UC is shut off and the fuel cell supplies the load independently. At $t = 70, 120$ and 160 seconds, the load power is suddenly reduced and the FC is providing more power than the required load power. The UC absorb over energy from the DC bus, inducing the increase of the SCs state as shown in Fig.7-f and Fig.8-f. While the fuel cell decreases slowly its output power to the new level of the load demand power. Furthermore, the UCs state of charge is well managed since, in steady state, UCs voltage tends to its reference value (24) and no energy is extracted for UCs ($i_{sc}(t)=0$).

These results demonstrate that the transient as well as the steady state load demand could be met. This whole approach is valid for both structures. It reveals and confirms the efficiency and performance of the control strategies. Thus, Both control strategies ensure the main objective of energy management in the hybrid system. But the comparison of the transient behavior of V_{BUS} and i_{FC} in both Figures shows that the second order SM can assure a smoother response shape than the first order, with continuous first derivative. Indeed, the major advantage of the second order SM is to avoid chattering and to provide smoother response, without losing the robustness and the reliability of the controller. In our case,

TABLE I
PARAMETERS OF HYBRID SYSTEM

FUEL CELL: PARAMETER NAME		Value
Open circuit voltage		45 V
Rated voltage		26 V
Rated current		46 A
ULTRACAPACITORS: PARAMETER NAME		Value
Capacitance		125 F
ESR		5.4 mΩ
Rated Voltage		30 V
Rated Current		200 A
Optimal Voltage (V_{UCref})		24 V
INDUCTORS & CAPACITIES: PARAMETER NAME		Value
Inductor L		100 μH
Rated Current L		150 A
Capacities C_{BUS}		14 mF

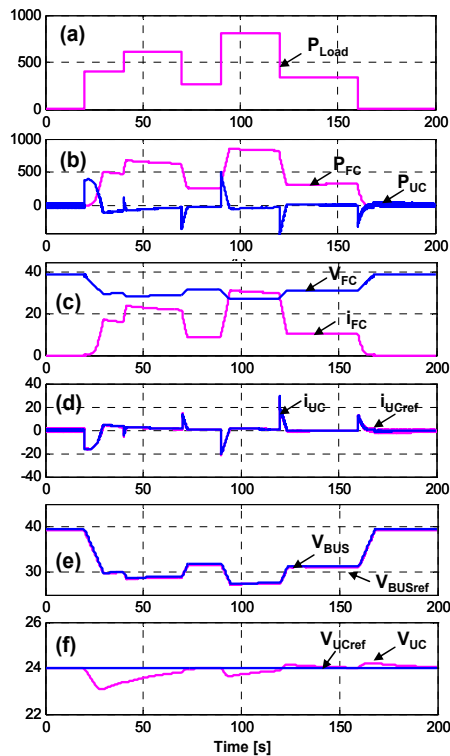


Fig. 7. Simulation results using SMC order I

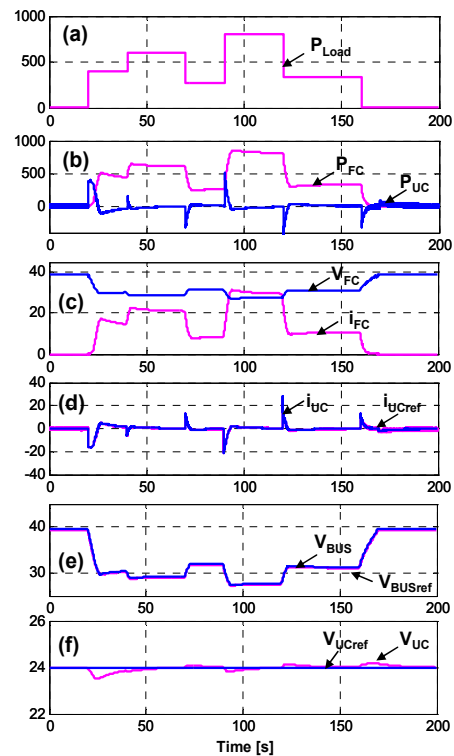


Fig. 8. Simulation results using SMC order II

the use of the integrator between u and V_{BUS} avoids chattering, but we still need the second order SM, given the requirements and the low dynamics of the fuel cell.

V. CONCLUSION

In this paper, a control strategy is developed for hybrid FC/UCs power source. Given the constraint of the FC dynamics and the complexity of the energy management. Two different strategies are designed using a first order and a second order sliding mode controller (SMC) to improve the robustness and the performance of the system. Simulation results clearly show that for both strategies, the performance of the system is improved, especially in the following aspects:

- Respect the slow dynamics of the fuel cell and guarantee the transient load by using the UCs.
- Maintain the state of charge of the UCs to its optimal.
- Assure the load requirements for even fluctuations.

Indeed, the major advantage of the second order SM is to avoid chattering and to provide smoother response, given the requirements and the low dynamics of the fuel cell.

REFERENCES

- [1] European Commission, Directorate-General for Research Information and Communication Unit, "European Fuel Cell and Hydrogen Projects 2002-2006," *European Communities*, EUR 22398, 2006, ISBN: 9279026925.
- [2] A. Emadi, Y.J. Lee, K. Rajashekara, "Power Electronics and Motor Drives in Electric, Hybrid Electric, and Plug-In Hybrid Electric Vehicles," *IEEE Trans. on Industrial Electronics*, Vol.55, No.6, June. 2008, pp. 2237-2245.
- [3] M. Ortúzar, J. Moreno, and J. Dixon, "Ultracapacitor-Based Auxiliary Energy System for an Electric Vehicle: Implementation and

- Evaluation", *IEEE Trans. on Industrial Electronics*, Vol.54, No.4, Aug. 2007, pp. 2147-2156.
- [4] F.N. Büchi, M. Inaba, and T.J. Schmidt, "Polymer Electrolyte Fuel Cell Durability", Springer, Feb. 2009, ISBN: 0387855343.I.S.
- [5] M.Gerardd, J-P. Poirot-Crouvezier, P. Schott, A.A. Franco, "PEMFC fuel cell/system interaction: analysis of the stack condition to minimize the oxygen starvation and impact on the fuel cell degradation performance", *Fundamentals and Developments of Fuel Cells Conference*, FDFC2008, Nancy, France, 2008.
- [6] M. Ehsani, Y. Gao, S.E. Gay, and A. Emadi, "Modern Electric, HybridElectric, and Fuel Cell Vehicles Fundamentals, Theory, and Design", *CRC Press*, 2005, ISBN: 0849331544.
- [7] V.A. Shah, J. A. Joshi, R. Maheshwari and R. Roy, "Review of Ultracapacitor Technology and itsApplications", *Fifteenth National Power Systems Conference (NPSC)*, IIT Bombay, Dec. 2008.
- [8] P. Barrade, A. Rufer, "The use of supercapacitors for energy storage in traction systems", *IEEE, Vehicular Power and Propulsion Symposium*, VPP'04, 6-8 Oct.2004.
- [9] F. Barbir, "PEM Fuel Cells", New York: Elsevier Academic Press, 2005.
- [10] F. Rafik, H.Gualous, R. Gallay, M.Karmous, and A.Berthon, "Contribution to the sizing of supercapacitors and their applications," *IEEE-ESCAP'04*. Conference, 2004.
- [11] P. Thounthong, S. Raël, and B. Davat, "Control strategy of fuel cell and supercapacitors association for distributed generation system," *IEEE, Transactions on Industrial Electronics*, Vol. 54, No. 6, Dec. 2008.
- [12] J.N. Marie-Francoise, H. Gualous, R. Outbib, and A. Berthon, "42V Power Net with supercapacitor and battery for automotive applications," *Journal of Power Sources*, Vol. 143, 2005, pp. 275-283.
- [13] T. Azib, O. Bethoux, G. Remy, C. Marchand, "Supercapacitors for Power Assistance in Hybrid Power Source with Fuel Cell," *IEEE-IECON'09*. Conference, 2009.
- [14] A. Levant, "Principles of 2-sliding modenext term design," *Automatica*, Vol. 43, Issue. 4, April. 2007, pp. 576-586.
- [15] M.K. Khan, S. Spurgeon, and A. Levant. Simple output-feedback 2 sliding controller for systems of relative degree two. In *European Control Conference ECC'03*, Cambridge, UK, 2003.
- [16] A. Levant, "Sliding order and sliding accuracy in sliding mode control," *Int. J. Control*, 58 :1247-1263, 1993.
- [17] R. Talj, Internal Rapport, *LGEP*, Sept. 2008.